



Published in final edited form as:

Lab Chip. 2011 September 7; 11(17): 2858–2868. doi:10.1039/c1lc20080a.

Microfiltration platform for continuous blood plasma protein extraction from whole blood during cardiac surgery

Kiana Aran^a, Alex Fok^a, Lawrence A. Sasso^a, Neal Kamdar^a, Yulong Guan^b, Qi Sun^b, Akif Ündar^b, and Jeffrey D. Zahn^a

Jeffrey D. Zahn: jdzahn@rci.rutgers.edu

^aBioMEMS Laboratory, Department of Biomedical Engineering, Rutgers, The State University of New Jersey, 599 Taylor Road, Piscataway, New Jersey, 08854, USA

^bPediatric Cardiovascular Research Center, Penn State Hershey College of Medicine, Penn State Hershey Children's Hospital, Hershey, Pennsylvania, USA

Abstract

This report describes the design, fabrication, and testing of a cross-flow filtration microdevice, for the continuous extraction of blood plasma from a circulating whole blood sample in a clinically relevant environment to assist in continuous monitoring of a patient's inflammatory response during cardiac surgeries involving cardiopulmonary bypass (CPB) procedures (about 400 000 adult and 20 000 pediatric patients in the United States per year). The microfiltration system consists of a two-compartment mass exchanger with two aligned sets of PDMS microchannels, separated by a porous polycarbonate (PCTE) membrane. Using this microdevice, blood plasma has been continuously separated from blood cells in a real-time manner with no evidence of bio-fouling or cell lysis. The technology is designed to continuously extract plasma containing diagnostic plasma proteins such as complements and cytokines using a significantly smaller blood volume as compared to traditional blood collection techniques. The microfiltration device has been tested using a simulated CPB circulation loop primed with donor human blood, in a manner identical to a clinical surgical setup, to collect plasma fractions in order to study the effects of CPB system components and circulation on immune activation during extracorporeal circulatory support. The microdevice, with 200 nm membrane pore size, was connected to a simulated CPB circuit, and was able to continuously extract ~15% pure plasma volume (100% cell-free) with high sampling frequencies which could be analyzed directly following collection with no need to further centrifuge or modify the fraction. Less than 2.5 ml total plasma volume was collected over a 4 h sampling period (less than one Vacutainer blood collection tube volume). The results tracked cytokine concentrations collected from both the reservoir and filtrate samples which were comparable to those from direct blood draws, indicating very high protein recovery of the microdevice. Additionally, the cytokine concentration increased significantly compared to baseline values over the circulation time for all cytokines analyzed. The high plasma protein recovery (over 80%), no indication of hemolysis and low level of biofouling on the membrane surface during the experimental period (over 4 h) were all indications of effective and reliable device performance for future clinical applications. The simple and robust design and operation of

these devices allow operation over a wide range of experimental flow conditions and blood hematocrit levels to allow surgeons and clinicians autonomous usage in a clinical environment to better understand the mechanisms of injury resulting from cardiac surgery, and allow early interventions in patients with excessive postoperative complications to improve surgical outcomes. Ultimately, monolithic integration of this microfiltration device with a continuous microimmunoassay would create an integrated microanalysis system for tracking inflammation biomarkers concentrations in patients for point-of-care diagnostics, reducing blood analysis times, costs and volume of blood samples required for repeated assays.

1. Introduction

A variety of hematological tests are commonly used for the rapid and accurate diagnosis and prognosis of medical conditions which promote immunological activation such as infectious diseases, autoimmune disorders, wound healing and trauma, as white blood cells continuously respond to pathological changes within the body.¹ Diagnostic blood protein analysis devices, typically require cell-free plasma, as the presence of cells such as RBCs can interfere with many detection systems for biochemical components of the blood.² Cells are typically removed and/or fractionated using chemical lysate buffers or centrifugation of a whole blood sample to separate cells from plasma based on density. More recently, significant research efforts have been made in microfluidic and miniaturized lab-on-a-chip blood analysis devices which can offer rapid analysis with minimal sample and reagent requirements.³ To date, many methods for particle and blood cell separations in microfluidic systems have been demonstrated. Some of these techniques have been applied to fractionate specific cell types or molecules from blood while other technologies are focused on efficient cell free plasma separation⁴ from blood samples for clinical analysis. Purely hydrodynamic microfluidic approaches to blood fractionation have been based on structuring of flow profiles based on microchannel design and geometry and/or operating flow conditions. These approaches are based on inertial force particle focusing,⁵ deterministic lateral displacement devices,^{6,7} hydrophoretic filtration,⁸ separation using the Zweifach–Fung effect,⁹ physical separation using microstructures^{2,3,10} and membrane filtration.^{11–13}

The purpose of the work described herein is to design and fabricate a low-cost plasma separation microdevice which can autonomously and continuously operate under a wide variety of blood hematocrit levels and clinical conditions. Devices using external fields as a separation modality, such as ultrasonic, electric and magnetic forces were discounted because they require the integration of piezotransducers, electrodes or magnets within the microfluidic device and their portability and versatility can be restricted.

Purely hydrodynamic separations are more attractive in this application because they do not require an external field and many different hydrodynamic approaches to blood cell fractionation and plasma separation from blood have been demonstrated. For example, separation of blood cell components, such as platelets and RBCs from diluted whole blood (2% blood in PBS) was accomplished using inertial flow fields in curved microchannels.⁵ Lateral migration of red blood cells which results in cell free plasma layers has also been used to separate plasma from whole blood. In one report using lateral migration, the channel geometry was modified in order to expand the dimension of the cell free region at high flow

rates of about 100 $\mu\text{l}/\text{min}$. However, the human blood was extremely diluted (1 : 20) in order to achieve extraction efficiency of about 10%.⁷ The Zweifach–Fung bifurcation law was also used to continuously separate plasma from whole blood, by controlling the flow rate ratio between a main blood channel and bifurcating plasma channels. The channels were specially designed so that cell centroids would always be beyond a bifurcating streamline separating the plasma channel and main channel flows so that plasma could be continuously ‘skimmed’ away from the device without cell contamination.⁹ Using this microdevice, which required accurate flow control through channel design dimensions, a plasma volume of 25% was collected but the volume percent of plasma collected decreased as blood hematocrit decreased. In another report, a better plasma yield (40%) was reported using Zweifach–Fung bifurcation law at very high flow rates (10 ml h^{-1}). However, purification efficiency of the plasma was low and the blood was extremely diluted (Hematocrit ~3%).¹⁴ In another device the Zweifach–Fung, Fahraeus and the pinched flow fractionation effect were combined to separate human plasma from red blood cells using a range of temperatures and flow rates. This device was reported to operate at high flow rates of up to 200 ml/min . However, the mean percentage of plasma collected in this device was about 3.5%.¹⁵ Another hydrodynamic separation approach termed hydrophoresis has been used to separate blood cells from plasma, by creating structured rotational flows with slanted structures and particle filters. Using the hydrophoresis principle 30% of plasma was collected from diluted (1 : 2 in PBS) rat blood.⁸

Other specially designed microstructures within microfluidic devices have been used to directly filter plasma from blood. For example, *in situ* polymerization was used to fabricate a microporous membrane within the microfluidic channel in order to separate plasma from diluted (1 : 20) rabbit whole blood placed in a hypotonic solution using dead-end filtration. However, the authors reported that only 20 μl of plasma volume could be collected before the device was completely clogged due to accumulation of blood cells.¹⁰ Alternatively, cross-flow filtration can be implemented to continuously clear particles from the filter surface, especially when dealing with complex fluids such as blood. In one report, a transverse-flow planar microfilter was designed to separate plasma from whole bovine blood based on capillary action. However, only a very small amount of plasma (maximum of 45 nl) was extracted after filtration and the quality of plasma was not tested since the plasma was not extracted from the device but significant hemolysis was observed as red coloration of the plasma.² Porous polymer membranes have been also used as the semipermeable barrier in cross-flow filtration devices. These filters are commercially available in different pore size and are very well suited for microfluidic blood applications as their pore size can be precisely selected at dimensions commensurate with blood cell exclusion. In one study, a microfilter with different types of commercially available porous polymer membranes was developed to separate plasma from whole blood.¹¹ However, while using this device, the filtrate showed evidence of hemolysis when the blood hematocrit was increased above 20% and fluid leakage around the filter was noted. Many of the technologies reported thus far have used diluted blood samples and may suffer from cell lysis, biofouling and/or clogging after some time and more importantly almost none of the reported blood separation microdevices have been tested in a clinical setting.

In order to overcome the challenges of plasma separation in a clinically relevant environment, we have developed a high throughput membrane-based cross-flow microfiltration microdevice to extract 100% cell-free plasma from blood over a wide range of hematocrit concentrations and does not require extensive blood dilution. A membrane based filtration approach was used in this project because the mass flux between microfluidic channels can be precisely controlled by incorporating membranes with various pore sizes in between the channels. The separation membrane is directly bonded as a laminated structure with aligned microfluidic channels so it can operate at high pressures with no evidence of membrane leakage or evidence of cell lysis or clogging over an extended period of operation (over 4 h).

The system developed in this study is intended to be used as a platform to track the concentrations of inflammatory biomarkers (complements and cytokines) within human blood during cardiac surgeries, especially when extracorporeal circulatory support also known as cardiopulmonary bypass (CPB) is used (about 400 000 adult and 20 000 pediatric patients in the United States per year).¹⁶ Although CPB revolutionized how cardiac surgeries are performed by allowing complicated valve replacement and cardiac repairs, especially of congenital defects in pediatric patients, coronary artery bypass grafts (CABG) and even heart transplants, the use of CPB is not without risks and adverse effects. CPB induces complex inflammatory responses characterized by complement, neutrophil, and platelet activation, endothelial dysfunction, and the release of proinflammatory cytokines. According to many studies, CPB procedures are responsible for initiation of a systemic inflammatory response syndrome (SIRS) that can result in a variety of post-operative complications.^{17–19} Studies have clearly shown significant correlations between the SIRS and several biomarkers including complement and cytokines.^{18,20,21} Characterization of a patient's blood plasma complements and cytokine concentrations during CPB procedures will allow researchers to identify the effects of CPB circuit components, pharmacological agents and surgical procedures on post-operative complications in order to reduce or prevent the effect of SIRS.²² Repetitive plasma samples are required to track the immune response during CPB procedures, which is only possible, using microfluidic systems with small sample volume requirements. Conventional blood sampling requires large blood volumes (>3 ml per vacutainer tube collected), but also involve multi-step sample handling processes (centrifugation, aliquoting, *etc.*) for analysis. The purpose of this study was to design and fabricate a disposable low-cost continuous plasma separation microdevice so that a sufficient volume of plasma (50–100 μ l) could be collected at the device outlet in a reasonable period of time (5–15 min) because this volume is required for conventional immunoassays. Using the microfiltration microdevice, it is possible to collect repetitive plasma samples as fractions, required for correlating inflammatory markers with short and long term post-operative complications.

2. Materials and methods

2.1. Design and fabrication

Microfluidic channels were fabricated in polydimethylsiloxane (PDMS) (Sylgard 184, Dow Corning, Midland, MI) using soft lithography.^{23,24} A chrome mask was used in contact

photolithography with negatively patterned SU-8 photoresist of varying thicknesses on a silicon substrate with PDMS molded against the SU-8 master. The filtration microdevice consists of two PDMS layers of microchannels, separated by a porous polycarbonate membrane (PCTE) (Nucleopore Polycarbonate Track-Etch Membrane, Whatman, Florham Park, NJ). Blood flows through the channels on one side of the device (reservoir channels) and blood plasma is filtered through the membrane and into the channels on other side of the membrane (filtrate channels). After a blood sample is introduced into the reservoir channel, the amount of purified plasma filtered across the membrane is based on the membrane pore size, the pressure in the reservoir channel and the relative flow resistances between the membrane and the reservoir and filtrate channel (similar to a simple electronic current divider). The pores in the membrane act as a steric barrier between large cellular components of blood and are only permeable to fluid and molecules smaller than its pore size. A schematic of cellular and molecular transport is shown in Fig. 1a. The reservoir channels were designed to be 600 μm wide and 135 μm deep, while the filtrate channels were designed to be 400 μm wide and 40 μm deep. Both channels were 25 mm long. In order to maximize the filtration area, the device was paralleled with 32 parallel channels in each layer to allow a high enough filtrate flow rate, in order to obtain 50 to 100 μl of plasma volume (which is required for blood analysis immunoassays) in a reasonable period of time (~15 min). The membrane was sandwiched between the two sets of aligned PDMS microchannels. The layers were bonded as a single laminate by surface modification of the polymer membrane *via* 3-aminopropyltriethoxysilane (APTES), followed by plasma activation of the PDMS microchannels as previously described.²⁵ Briefly, the PCTE membrane was activated in an oxygen plasma chamber for 1 min (600 mTorr, 100 W) and then immersed in a 5% APTES solution at 80 $^{\circ}\text{C}$ for 20 min. The membrane then was removed from the APTES solution and was placed on a cleanroom wipe to dry. The surface of a fully cured PDMS microdevice and the APTES modified membrane were activated in an oxygen plasma chamber (600 mTorr, 100W) for 20 s. The membrane and the treated microdevice were brought into contact and an immediate irreversible bond was formed. In order to bond the membrane to the second PDMS layer in a sandwich structure, the first bonded laminate and a second PDMS layer were similarly activated in an oxygen plasma chamber, aligned, brought into contact and subsequently pressed together. A schematic of the sandwich structure is shown in Fig. 1b. The reservoir and filtrate channels were designed with varying widths so that the two layers could be aligned by hand, having the two sets of channels still overlap while accommodating alignment errors.

2.2. The effects of blood hematocrit and membrane poresize on plasma separation efficiency

In order to maximize the microfiltration efficiency in the proposed microdevice, it was necessary to understand the transport mechanism through the membrane. A significant problem often encountered with membrane-based filtration devices for blood separation is protein biofouling on the membrane surface, and the high deformability of red blood cells which may lyse and/or clog the membrane pores and reduce the filtrate flux across the membrane. This requires an understanding of balancing the need to have a high filtrate flow rate for sample collection by modifying the membrane poresize with the propensity of higher flow rates to produce membrane clogging. Additionally, the level of blood

anticoagulation also affects protein and cellular absorption to the membrane. Heparin is widely used in clinical environments as an anticoagulant to prevent blood clots from forming. The amount of heparin administered can vary depending upon clinical guidelines from light administration to patients in an emergency department or hospital room, medium levels to patients on extracorporeal life support or high doses during cardiac surgeries requiring CPB. The quantity of heparin administered is also adjusted according to coagulation test results to make sure the level of anticoagulation is in the required therapeutic range. Additionally, heparin is commonly used to coat blood contacting devices to create a non-thrombogenic surface and for maintaining blood fluidity during blood handling procedures.

To explore the effect of membrane flow resistance and blood hematocrit (Hct) level using the microfiltration device, experiments were performed by infusing lightly heparinized sheep blood of varying hematocrit through the reservoir of the device. Sheep's blood was chosen because of its low cost and its availability from reliable suppliers. However, sheep's blood rheology varies from that of human²⁶ and this can affect the plasma separation efficiency of the device. Whole sheep's blood (42% Hct, heparinized to 300 IU/L heparin to prevent blood coagulation during shipping) was obtained from a scientific vendor (Hemostat Labs, Dixon, CA), and was used for experiments within two weeks of harvest. The blood was hemodiluted to 34%, 30% and 20% hematocrit by addition of Lactated Ringers solution (Baxter Healthcare Corp, Deerfield, IL) with the hematocrit verified using a Coulter cell and particle counter (Beckman Coulter Inc., Hialeah, FL, USA). The filtration capacity of the device was then investigated using a microfiltration device with a 200 nm PCTE membrane and infusing blood through the reservoir channels at a constant flow rate of $80 \mu\text{l min}^{-1}$ over a 2 h experimental period. At this flow rate, the average shear stress in the reservoir was estimated as $\mu_{\text{blood}} \times U/H = 4.27 \text{ dynes/cm}^2$ where μ_{blood} is the viscosity of the blood ($3.5 \times 10^{-3} \text{ Pa}\cdot\text{s}$), U is the average velocity of the blood in the reservoir channels ($1.65 \times 10^{-2} \text{ m s}^{-1}$) and H is the channel height (135 μm). This is 200 times smaller than the critical shear stress required for shear induced RBC hemolysis.²⁷ Discrete blood samples were collected as fractions from both the reservoir and filtrate outlets every 20 min and the collected filtrate volumes were measured at each time point to identify any reduction in filtrate flow rate due to membrane clogging. Additionally, in order to optimize device performance, the effects of membrane pore-size on plasma separation was studied. In this experiment, devices were fabricated using PCTE membranes with either 100 nm or 200 nm pore diameters and the filtration flow rate between the two types of membranes was compared.

As an approach to maintain the filtrate flow rate over time, especially at high hematocrit levels, some microdevices were pre-infused with heparin as an anticoagulant. Therefore, the microdevice was infused with 1000 IU/ml (2 mg of sodium heparin in 1 ml of Lactated Ringer's solution) for at least 30 min prior to infusing blood into the microdevice, in order to reduce the amount of platelet adhesion to the surface of the membrane. The filtration flow rate over time between pre-coated and non-coated microdevices were then compared.

Following each blood experiment, the microfiltration devices were cut using a razor blade, and a small piece of membrane was removed. The membranes were then fixed in 2% glutaraldehyde, dehydrated, and inspected using scanning electron microscopy

(AMRAY-1830I, AMRAY, Bedford, MA) to examine the membrane surface for indications of cellular or protein absorption after being exposed to blood.

2.3 Membrane biofouling due to APTES treatment

The polycarbonate membranes used in this study were reported by the manufacturer to be hydrophilic and low in protein adsorption. However, since the membranes surface were modified *via* APTES in order to create the laminated structures, it was critical to identify any unfavorable biological interactions or excessive protein adsorption due to APTES treatment, which could potentially alter the membrane filtration properties. In order to study protein adsorption occurring at the membrane surface, a Quartz Crystal Microbalance with Dissipation monitoring (QCM-D) (Q-Sense, Goteborg, Sweden) and gold coated quartz crystals with fundamental resonant frequency of 5 MHz and a diameter of 14 mm were used. QCM-D is a well suited technology for dynamic monitoring of the absorbed protein mass onto material surfaces.^{28,29} The crystals were cleaned prior to experiments by soaking them in tetrahydrofuran (THF) for 15 min followed by exposure at 80 °C to a 5 : 1 : 1 by volume mixture of distilled water, ammonium hydroxide and hydrogen peroxide for 15 min. The quartz crystals were then thoroughly rinsed with deionized water and gently blown dry under a flow of nitrogen gas and placed in a UV chamber for 10 min. The gold side of each crystal was then coated with 50 nm of 1% w/v polycarbonate polymer solution in chloroform (Fisher Scientific) and left in a vacuum chamber for 24 h. Two polycarbonate coated crystals were mounted in two separate QCM-D flow chambers with the coated surface exposed to the solution and a stable baseline response of the quartz crystals in water at 80 °C was established. In preparation for adsorption of APTES modified surface, 5% APTES solution (prewarmed to 80 °C prior to use) was perfused through one flow chamber, at a high flow rate of 0.117 ml min⁻¹ (in order to maintain the 80 °C temperature for polymer-APTES interaction) for 20 min while water was still perfused through the other flow chamber. This procedure of treating the polycarbonate coated crystals with APTES was similar to the procedure carried out to treat the polycarbonate membranes in the fabrication of the microdevices. The system was then left to cool down and stabilized at 35 °C (normothermia). In order to compare the adsorption of protein into both APTES treated and non-coated crystals, first phosphate buffered saline (PBS) was perfused through both chambers for 20 min and then sheep's blood plasma was perfused through the system at a flow rate of 80 µl min⁻¹ for 20 min. Desorption was performed immediately after the adsorption reached steady state by replacing the plasma solution with PBS solution and the final frequency change at each time point was measured in the presence of PBS after it reached the steady state. This procedure was repeated 4 times to study protein adsorption over time. The kinetics of plasma protein adsorption and desorption were followed by changes in resonant frequency and dissipation.

In order to obtain the thickness of the adsorbed protein layer, raw frequency and dissipation data obtained from QCM-D were experimentally fit to a Voigt model described by Voinova *et al.*,³⁰ using the supplied software. According to this model the relationship between the frequency and dissipation shifts (Δf and ΔD) can be fit to the following equations:

$$\Delta f \approx \frac{1}{\pi \rho_0 h_0} \left\{ \frac{\eta_3}{\delta_3} + h_1 \rho_1 \omega - 2h_1 \left(\frac{\eta_3}{\delta_3} \right)^2 \frac{\eta_1 \omega^2}{\mu_1^2 + \omega^2 \eta_1^2} \right\}$$

$$\Delta D \approx \frac{1}{\pi f \rho_0 h_0} \left\{ \frac{\eta_3}{\delta_3} + 2h_1 \left(\frac{\eta_3}{\delta_3} \right)^2 \frac{\eta_1 \omega}{\mu_1^2 + \omega^2 \eta_1^2} \right\}$$

In these equations the viscoelastic properties of the protein layers are represented as four parameters: layer density (ρ_1) viscosity (η_1), shear elasticity (μ_1) and thickness (δ_1). (ρ_0 , h_0) are crystal density and thickness, (ρ_3 , η_3 , δ_3) are liquid density, viscosity and thickness and ω is the angular frequency of oscillation. The fixed parameters used in the experimental fitting were (i) layer density $\rho_1 = 1200 \text{ kg m}^{-3}$ (density of the layer should lie approximately between that of protein layer (1400 kg m^{-3})³¹ and trapped water (1000 kg m^{-3})), (ii) fluid viscosity $\eta_3 = 0.001 \text{ Pa s}$, and (iii) fluid density $\rho_3 = 1000 \text{ kg m}^{-3}$. The fitted parameters were (i) layer viscosity between $\eta_1 = 0.0005\text{--}0.01 \text{ Pa s}$, (ii) layer shear modulus between $\mu_1 = 10^4\text{--}10^9 \text{ Pa}$, and (iii) layer thickness between $\delta_1 = 0\text{--}5 \times 10^{-7} \text{ m}$. The mass of protein adsorbed can then be calculated using the calculated layer density and thickness.

2.4. Blood protein separation using the microfiltration microdevice in a simulated CPB circuit

The performance of the microdevice was evaluated during an experiment using heparinized fresh human blood, with an *in vitro* model CPB circulation loop (Fig. 2a) which is identical to conditions used during cardiac surgeries (minus the patient). The simulated extracorporeal circuit consisted of an HL-20 heart-lung machine with a multifold HL-20 Roller blood pump (Jostra HL-20, Jostra, Austin, TX), a hollow fiber pediatric oxygenator with an integrated heat exchanger module (Capiiox RX 05RW Terumo Corporation, Tokyo, Japan), a 32 μm Capiiox pediatric arterial filter (CX*AF02; Terumo Corporation, Tokyo, Japan), a pediatric venous reservoir with an integrated cardiectomy filter (Capiiox cardiectomy reservoir CX*CR10NX), and a MAQUET Heater-Cooler (Jostra Heater-Cooler Unit HCU 30 Houston, TX). In order to simulate the systemic vasculature resistance from a patient, a Hoffman clamp was tightened distal to a second reservoir which simulated our 'pseudo patient' at clinically relevant circuit pressure and pump flow rate. Pulmonary and aortic resistances were controlled *via* a series of pinch clamps. A schematic of the extracorporeal circuit is shown in Fig. 2a.

The CPB circulation loop was primed with 500 ml of heparinized fresh human blood, drawn from healthy adult volunteers and brought into the lab within 30 min of collection. The significance of the effect of blood age on immune activation has been previously documented and therefore fresh blood was chosen because it shows a significantly larger amount of immune activation than older blood products.³² The blood was hemodiluted to ~27%–30% hematocrit in Lactated Ringer's solution and heparinized up to ~5000 IU/blood bag (each blood bag contains between 300–500 ml of blood) consistent with surgical anticoagulation protocols. Hemodilution using crystalloid solution during CPB is a common procedure due to the required extracorporeal circuit priming volume and the limitation in donor blood availability from blood banks. It also reduces blood viscosity and improves microcirculatory flow. The blood was then circulated at a rate of 500 ml min^{-1} at an arterial

circuit pressure of 100 mmHg. Nonpulsatile perfusion was performed and the temperature was set at normothermia (35 °C) for the duration of the experiments. After complete mixing of the blood and prime fluid was accomplished, a small portion of the blood was redirected from the arterial port of the membrane oxygenator to the microfiltration device without any further modification. Fig. 2b shows a picture of the device being infused with human blood. The reservoir flow rate of the microdevice was approximately $80 \mu\text{l min}^{-1}$, driven by pressure from the circulation circuit. The fluid fractions from both microdevice outlets of the reservoir and filtration channels were collected in 20 min intervals for a total circulation time of 4 h. Discrete blood samples of 1 ml volume were also collected from the arterial port of the membrane oxygenator as a control sample. Following collection, the direct draw and reservoir blood samples were centrifuged; the plasma was removed and snap frozen at $-80 \text{ }^\circ\text{C}$ on dry ice until analyzed. Finally the device was cut and a small piece of membrane was removed, fixed in 2% glutaraldehyde, dehydrated, and inspected using scanning electron microscopy (AMRAY-1830I, AMRAY, Bedford, MA) to evaluate the membrane surface after being exposed to human blood. The concentration of inflammatory cytokines (TNF- α , IL-1 β , IL-6, and IL-8) were measured using a human inflammatory cytokine cytometric bead assay (CBA) kit (BD Biosciences, San Jose, CA, USA) according to the manufacturer's instructions. The plasma samples were used as collected without any dilution. Briefly, the cytometric assay beads were mixed, washed, and resuspended in a serum enhancement buffer. Following bead preparation, 50 μl of the calibration and collected blood samples were mixed with 50 μl of bead solution and incubated for 1.5 h. Following incubation, the beads were diluted in 1 ml of wash solution, centrifuged and then all but 100 μl of wash solution was gently removed from each tube. 50 μl of human inflammatory phycoerythrin (PE) labeling agent was then added to each tube and mixed with the beads which were resuspended by gentle agitation. The labeling agent was incubated for 1.5 h followed by another bead washing procedure and centrifugation and finally resuspending the beads in 300 μl of buffer for analysis. The bead fluorescence intensities were evaluated using a BD FACSCalibur flow cytometer and compared to calibration intensities of known standard solutions for quantifying cytokine concentrations. The cytometric bead assay is a multiplexed assay by isolating beads for analysis *via* their FSC and SSC signal and each cytokine is delineated by the bead FL3 channel intensity where each bead corresponding to a particular cytokine produces a different FL3 intensity separating individual bead populations for each cytokine of interest. The cytokine concentration quantification is based on the bead FL2 intensity where the bead intensity using this channel is proportional to the cytokine concentration.

3. Results and discussions

3.1. The effects of blood hematocrit level on microdevice performance

Ensuring reliable operation of the device over a wide range of blood hematocrit levels and anticoagulation levels is an important factor in extending the performance of the device. The filtration efficiency of the device was evaluated using sheep's whole blood. However, the device efficiency can vary with blood from different species, because the changes in blood rheological behavior may result in the change of adhesion of cells and proteins to the membrane surface. For example, the size of the sheep RBCs (average diameter of 4.8 μm)

varies from that of human (average diameter of 6–8 μm). This can alter the device performance to a degree. Additionally high concentration of cellular components (high hematocrit) increases the pressure across the device, which can result in clogging of the membrane pores by blood cells. To assess the effect of blood hematocrit on the filtration capacity of the device, the volumetric flow rates at the filtrate outlet were measured over time at various hematocrit levels with whole sheep's blood infused into the inlet of the reservoir channels. The absolute reservoir and filtrate flow rates varied between experiments due to changes in blood rheology which can vary between different blood batches as well as differences in membrane pore density which can vary greatly between membrane batches (indicated as between 1×10^5 to 6×10^8 pores/ cm^2 by the manufacturer). However, a consistent trend seen over several ($n = 5$) experiments is that the permeate flux flow rate directed to the plasma outlet decreased over time using whole blood at high hematocrit levels (~42%). However, tests with blood at various lower Hct. in the range of 20% to 34% showed that the plasma separation was efficient and did not decrease significantly over the duration of the experiments. Also, at higher hematocrit levels the filtrate flow rate was initially larger due to higher reservoir pressure induced by higher viscosity of the blood. However, the flow across the membrane decreased quickly due to the accumulation of red blood cells or adhesion of platelets at the membrane surface. Representative experimental results, obtained using one batch of blood over a set of experiments is shown in Fig. 3a.

High quality filtration of blood cells can be achieved using a membrane with relatively small pores, which requires high pressure for driving the plasma through the filter. High pressure can be problematic at high cell concentration as large cells are pushed into the membrane pores. Comparison of the performance of microfiltration devices with 200 nm and 100 nm membranes (both suitable for plasma separation purposes) indicated that at a high hematocrit level, the initial filtrate flow rate is higher using 200 nm because it is less resistive to the flow. However, the filtrate flow rate decreases faster over time as it is easier for large cells to enter and clog the pores (Fig. 3b).

To improve the device performance at high hematocrit levels using a 200 nm membrane pore size, the surface of the microdevice was pre-coated with an anticoagulant (heparin) in order to decrease the amount of cell adhesion on the membrane surface. When using sheep blood at high Hct levels (39% as received), the filtrate flow rate did not change significantly over time for the heparin coated microdevice but decreased rapidly and significantly using the non-coated device (Fig. 3c).

Finally, a 200 nm membrane was chosen for *in vitro* CPB experiments because it provided higher plasma volume and its filtrate flow rate did not significantly change during *in vitro* human blood filtration experiments.

3.2. Protein mass adsorption to polycarbonate with and without APTES coating

The typical adsorption of plasma proteins onto the polycarbonate-coated crystal surface was monitored, with and without APTES modification, in real time, by simultaneously measuring of f_s and D_s using QCM-D. Fig. 4a shows a schematic diagram of the protein adsorbed to the polycarbonate polymer on a quartz crystal surface. Fig. 4b and 4c show the representative fifth harmonic f_5 and D_5 for both APTES modified and unmodified

polycarbonate which displayed the best experimental fit to theory, as functions of time when the QCM-D is alternately exposed to plasma and PBS solutions. The arrows indicate the injection time of plasma, and the labels time 1 through time 4 indicate several periods of rinsing steps using PBS. Protein adsorption caused a rapid initial frequency decrease (mass increase) accompanied by a dissipation factor increase at the same rate, until the protein adsorption saturated when a slower frequency change was observed. After exchanging the plasma solution with PBS to remove the non-adherent proteins, the frequency increased again. The actual mass adsorbed to the surface was measured when the system response stabilized during PBS exposure. Fig. 4d shows the calculated mass adsorbed to the surface of APTES treated and untreated polycarbonate polymer on the quartz crystal obtained from the QCM-D data. The mass of protein initially adsorbed on polycarbonate material was about 0.97 ng m^{-2} , whilst the mass adsorbed on APTES treated polycarbonate material was approximately 20% higher. However, the small standard deviation for both the APTES treated ($\sigma = 0.04$) and non-treated ($\sigma = 0.09$) crystal surfaces, indicated a small degree of variation in the mass of the protein layer adsorbed over time. It is also important to note that the mass estimated by Voigt model from QCM-D includes the mass of both protein and any water that is trapped within the protein layer so that pure mass of protein is not easily quantified. In the actual devices, the extent of protein adsorption and cell adhesion also depends on the flow conditions where at higher blood flow rates the fluid shear helps prevent protein buildup.

3.3. Blood proteins separation using microfiltration microdevice

The ability of the microfiltration device to perform continuous separation of blood proteins from whole blood was characterized using the Penn State pediatric CPB simulated model. When using a 200 nm pore size, about 15% of the total blood volume was collected in the filtrate channels without any contaminating blood cells or indications of RBC hemolysis. Although no quantitative hemoglobin concentration quantification of the collected filtered plasma was conducted, each sample collected was clear with a slightly yellow tinge as is commonly seen in the plasma fractions of blood following centrifugation indicating only minimal hemolysis of red blood cells. Blood samples were also collected from the device reservoir, as well as a direct draw control sample, centrifuged to remove the cellular components, and stored at $-80 \text{ }^{\circ}\text{C}$ for subsequent assaying to investigate the effect of the CPB circuit on immune activation. Fig. 5(a–d) shows the temporal change in cytokine concentrations over a 4 h circulation time for samples collected from both the reservoir and filtrate outlets using the microfiltration device and were comparable to those measured from the direct blood draw. Results from conducting a pair wise t-test at each sampling time compared to baseline cytokine concentration indicated that the cytokine concentrations for all groups tested increased significantly over the circulation time ($p < 0.01$). Table 1, shows the Pearson's correlation coefficient (r) calculated between both the reservoir and direct draw sample and the filtrate and direct draw sample, indicating a high level of recovery of cytokines ($r > 0.99$ for all samples) using the microfiltration device.

Finally, a comparison was done to quantify the cytokine recovery compared to the direct blood draw. At each time point, the measured cytokine concentration from the reservoir and

filtrate outlets were normalized to the direct draw concentration and compared to each other. For all samples tested the recovery was greater than 80% (Fig. 5e).

3.4. SEM evaluation of blood contacting membranes

SEM images of the membranes are useful to assess the degree of protein or cellular absorption which can produce biofouling of the membrane causing a decline in the filtration flux across the membrane over time. Fig. 6 shows SEM images of a 200 nm membrane prior to blood exposure (Fig. 6a) and after exposure to both heavily heparinized (~5000 IU/blood bag) human blood (Hct = 27–30%) (Fig. 6b) and lightly heparinized (~300 IU/L) sheep's blood (Hct~30%) (Fig. 6c). The SEM image of a 200 nm membrane after exposure to human blood during CPB procedure, showed little protein absorption and did not indicate any platelet adhesion. Contrarily, the SEM image of the membrane following exposure to sheep's blood revealed that at high hematocrit levels, protein and platelet adhesion was significant, most likely due to the lower amounts of anticoagulant used in the sheep's blood. Additionally the filtration flow rate ($\sim 10 \mu\text{l min}^{-1}$) was higher during CPB experiments using human blood than the flow rate ($\sim 3 \mu\text{l min}^{-1}$) during bench-top experiment using sheep's blood, despite the fact that the blood inlet flow rate was the same for both experiments ($\sim 80 \mu\text{l min}^{-1}$). However, the filtrate volume did not decrease over time in either experiments. The effects of blood anticoagulant were investigated when using blood at high hematocrit levels by pre-coating the devices with heparin as is commonly done in blood collection vials in order to reduce protein and cellular adhesion to the membrane surface. Comparison between the SEM images of a non-coated membrane (Fig. 6d) and a heparin pre-coated membrane (Fig. 6e) after exposure to lightly heparinized (~300 IU/L) sheep's blood (Hct = 39%) indicated a significant decrease in cellular adhesion to the membrane surface of the pre-coated membrane. The results from SEM images, along with the results from filtration efficiency over time for anticoagulant pre-coated microdevice, demonstrate this approach is useful for maintaining the filtration efficiency over time without the need to add heparin systemically to the blood sample. The results also indicated that pre-coating the microfiltration device with a sufficient amount of anticoagulant can expand its applications to all blood Hct concentrations at any level of anticoagulation.

4. Conclusions and future work

This work demonstrated the design, fabrication and testing of a microfiltration device used for the selective separation of blood proteins from whole blood in a clinically relevant environment. The microfiltration device was fabricated by using two PDMS layers of microchannels and a polycarbonate (PCTE) porous membrane with low protein adsorption which enabled its utilization of complex fluids such as blood. The device performance was evaluated by using both sheep's blood in benchtop analysis and heparinized freshly drawn human blood within a simulated normothermic CPB circuit. However, a study on the extent of hemolysis and plasma purity at different Hct levels and inlet flow rate is not included in this work, and although the plasma is 100% cell free, further studies need to be undertaken to quantify the hemoglobin concentration in the filtrate to better evaluate the extent of hemolysis.

The results also indicated that the pre-coated microdevice has the potential to be used during various clinical application, where lower levels of anticoagulant might be used due to bleeding complications associated with extensive use of anticoagulants, such as extracorporeal life support (ECLS). The anticoagulant pre-coated microdevice is currently being studied using an animal ECLS model to evaluate its performance in another clinically relevant environment.

Additionally, the microfiltration device is being monolithically integrated with a microfluidic immunoassay which can measure protein concentration at a high sampling rate.³³ The microfiltration device provides a continuous stream of cell-free blood plasma to the immunosensor, which would otherwise become clogged if whole blood were infused into it. This integrated microfiltration/immunoassay device will enable a thorough characterization of the inflammation caused by CPB procedures, as well as offering real-time measurements of inflammation during surgery.

Acknowledgments

This work (JDZ) was supported by the National Institutes of Health National Heart Lung and Blood Institute grant No. 1R21HL084367-01A1 and Wallace H. Coulter Foundation Early Career Translational Research Awards in Biomedical Engineering. The authors also wish to thank Joachim Kohn and Arnold Luk for QCM-D discussions and use of the equipment.

Notes and references

1. Toner M, Irimia D. *Annu Rev Biomed Eng.* 2005; 7:77–103. [PubMed: 16004567]
2. Crowely TA, Pizziconi V. *Lab Chip.* 2005; 5:922–929. [PubMed: 16100575]
3. Van Delinder V, Groisman A. *Anal Chem.* 2006; 78:3765–3771. [PubMed: 16737235]
4. Mukherjee S, Kang T, Chen Y, Kim S. *Crit Rev Biomed Eng.* 2009; 37:517–529. [PubMed: 20565382]
5. Di Carlo D, Edd JF, Irimia D, Tompkins RG, Toner M. *Anal Chem.* 2008; 80:2204–2211. [PubMed: 18275222]
6. Huang LR, Cox EC, Austin RH, Sturm JC. *Science.* 2004; 304:987–990. [PubMed: 15143275]
7. Sollier E, Rostaing H, Pouteau P, Fouillet Y, Luc Achard J. *Sensors and Actuators B.* 2009; 141:617–624.
8. Choi, S.; Park, J-K. *Solid-State Sensors, Actuators and Microsystems Conference, 2007. TRANSDUCERS 2007. International; 2007; p. 1769-1772.*
9. Yang S, Undar A, Zahn JD. *Lab Chip.* 2006; 6:871–880. [PubMed: 16804591]
10. Moorthy J, Beebe DJ. *Lab Chip.* 2003; 3:62–66. [PubMed: 15100783]
11. Thorslund S, Klett O, Nikolajeff F, Markides K, Bergquist J. *Biomed Microdevices.* 2006; 8:73–79. [PubMed: 16491334]
12. Gu Y, Miki N. *J Micromech Microeng.* 2007; 17:2308–2315.
13. Gu Y, Miki N. *J Micromech Microeng.* 2009; 19:065031.
14. Kersaudy-Kerhoas M, Dhariwal R, Desmulliez MPY, Jovet L. *Microfluid Nanofluid.* 2010; 8:105–114.
15. Rodriguez-Villarreal AI, Arundell M, Carmona M, Samitier J. *Lab Chip.* 2010; 10:211–219. [PubMed: 20066249]
16. Adult Cardiac Surgery Database, Congenital Heart Surgery Database. [Accessed March 25, 2011] <http://www.sts.org/national-database/database-managers/executive-summaries>
17. Miller BE, Levy JH. *J Cardiothorac Vasc Anesth.* 1997; 11:355–366. [PubMed: 9161905]
18. Moore FD, Warner KG, Assousa S. *Ann Surg.* 1988; 208:95–103. [PubMed: 3260474]

19. Wan S, LeClerc JL, Vincent JL. *Chest*. 1997; 112:676–692. [PubMed: 9315800]
20. Levy JH, Tanaka KA. *Ann Thorac Surg*. 2003; 75:S715–S720. [PubMed: 12607717]
21. Steinberg JB, Kapelanski DP, Olson JD, Weiler JM. *J Thorac Cardiovasc Surg*. 1993; 106:1008–1016. [PubMed: 8246532]
22. Westaby S. *Intensive Care Med*. 1987; 13:89–95. [PubMed: 3553271]
23. Duffy DC, McDonald JC, Schueller OJA, Whitesides GM. *Anal Chem*. 1998; 70:4974–4984. [PubMed: 21644679]
24. Xia YN, Whitesides GM. *Annu Rev Mater Sci*. 1998; 28:153–184.
25. Aran K, Sasso LA, Kamdar N, Zahn JD. *Lab Chip*. 2010; 10:548–552. [PubMed: 20162227]
26. Windberger U, Bartholovitsch A, Plasenzotti R, Korak KJ, Heinze G. *Exp Physiol*. 2003; 88:431–440. [PubMed: 12719768]
27. Hellums JD. *Ann Biomed Eng*. 1994; 22:445–455. [PubMed: 7825747]
28. Höök F, Rodahl M, Brzezinski P, Kasemo B. *Langmuir*. 1998; 14:729–734.
29. Johnson PA, Luk A, Demtchouk A, Patel H, Sung H-J, Treiser MD, Gordonov S, Sheihet L, Bolikal D, Kohn J, Moghe PV. *Journal of Biomedical Materials Research Part A*. 2010; 93A:505–514. [PubMed: 19585568]
30. Voinova MV, Rodahl M, Jonson M, Kasemo B. *Phys Scr*. 1999; 59:391–396.
31. Höök F, Vörös J, Rodahl M, Kurrat R, Böni P, Ramsden JJ, Textor M, Spencer ND, Tengvall P, Gold J, Kasemo B. *Colloids Surf, B*. 2002; 24:155–170.
32. Aran K, Fok A, Guan Y, Sun Q, Zahn JD, Ündar A. *Artificial Organs*. 2010; 34:1048–1053. [PubMed: 21137157]
33. Sasso L, Ündar A, Zahn J. *Microfluidics and Nanofluidics*. 2010; 9:253–265. [PubMed: 20694166]

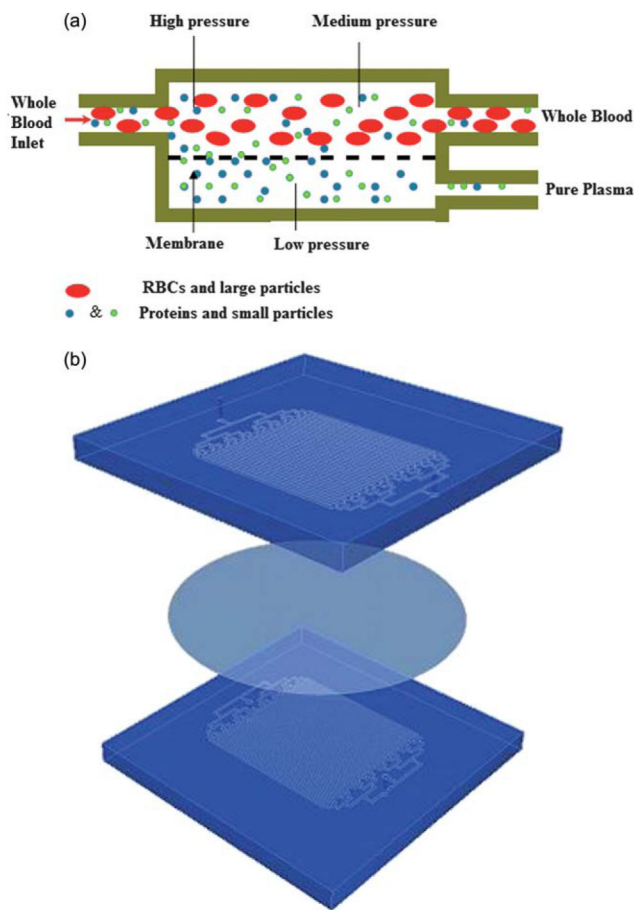


Fig. 1. Schematic illustrations showing the microfiltration design and transport mechanism. (a) Schematic of the two compartment microfiltration device. The top compartment is a reservoir channel. The bottom channel is a filtrate channel where plasma flows across a semipermeable membrane from the reservoir into the filtrate channels. (b) The activated membrane and PDMS layers are bonded together to form a sandwich structure.

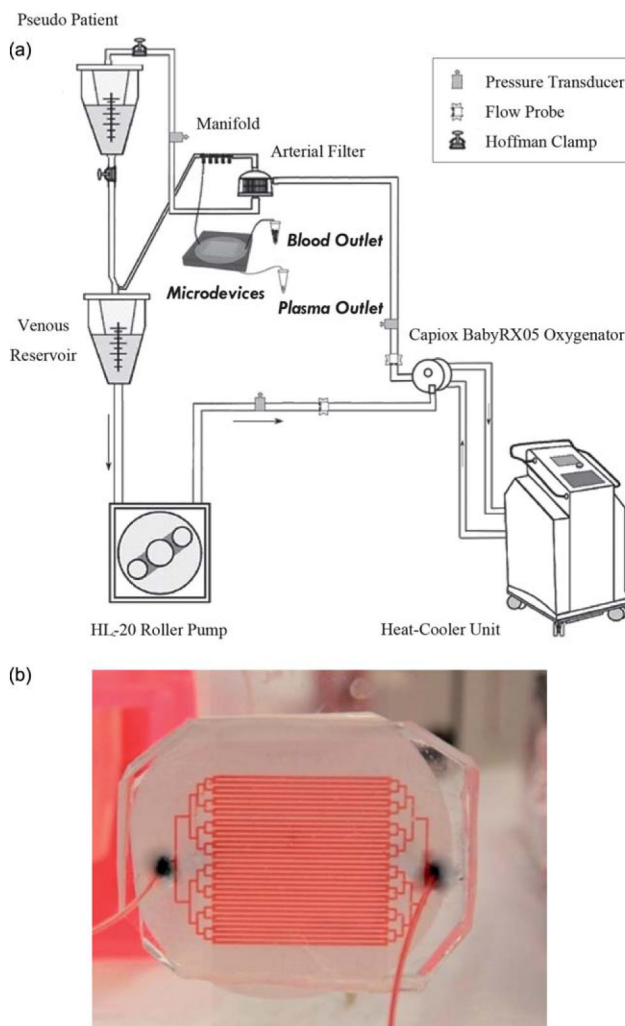
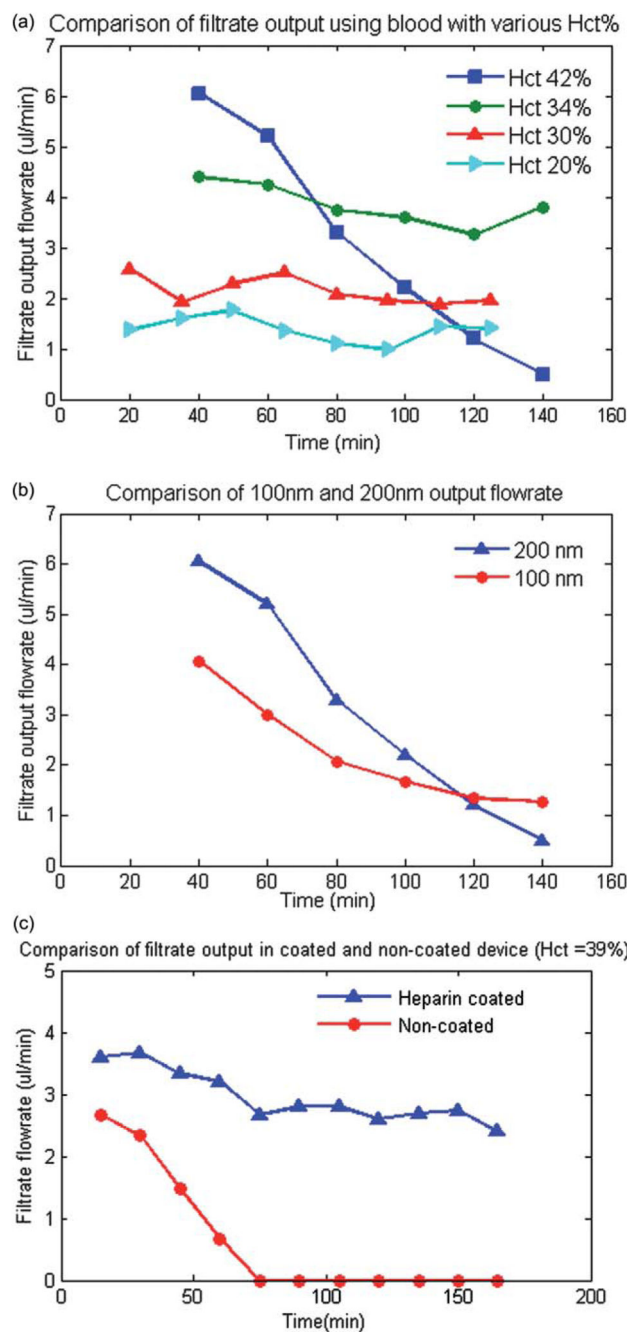


Fig. 2. (a) A schematic of the extracorporeal circuit including the roller pump, oxygenator, arterial filter and venous reservoir. The circuit is fed to a blood reservoir which represents the pseudo-patient with the systemic circulation resistance modeled by the tightening of a Hoffman clamp. The inlet of the microfiltration device is connected to a manifold at the arterial port of the oxygenator. (b) A picture of the device while being perfused with blood.

**Fig. 3.**

(a) A comparison of the experimental results of the total plasma separation flow rate with respect to blood inlet hematocrit level. The results indicate that initial filtration flow rate is higher for high level of hematocrit (42%) but it decreases rapidly due to accumulations of RBCs or platelet at the surface of the membrane. (b) A comparison of the plasma separation flow rate for 100 nm and 200 nm pore size membrane. The results indicates that the plasma flow rate is higher for 200 nm membrane. However, the flow rate decreases more rapidly over time for 200 nm membrane at hematocrit levels of 42%. (c) A comparison of the

experimental results of the total plasma separation for anticoagulant coated and non-coated microdevice for blood Hct = 39% indicated that the filtration efficiency did not significantly decrease over time for the heparin pre-coated device but it decreased significantly for the non-coated device.

Author Manuscript

Author Manuscript

Author Manuscript

Author Manuscript

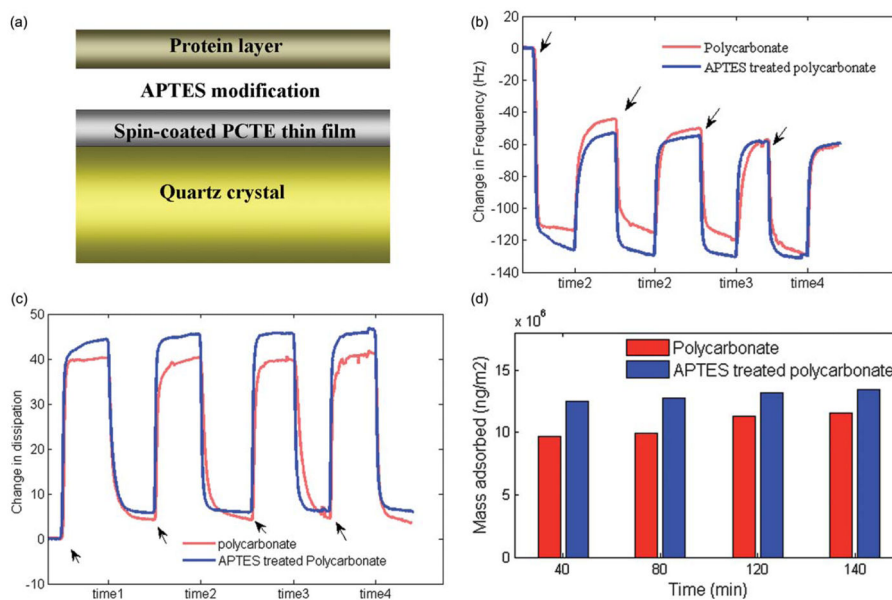


Fig. 4. (a) A schematic diagram of the protein polymer adsorption on a quartz crystal surface. (b) Frequency shift (Δf) and (c) dissipation shift (ΔD) induced by the adsorption of plasma proteins as a function of time. (d) Mass adsorbed to the surface of APTES treated and non-treated polycarbonate polymer on quartz crystal which indicates no significant change in the amount of protein adsorption over time for both APTES modified and unmodified polycarbonate material.

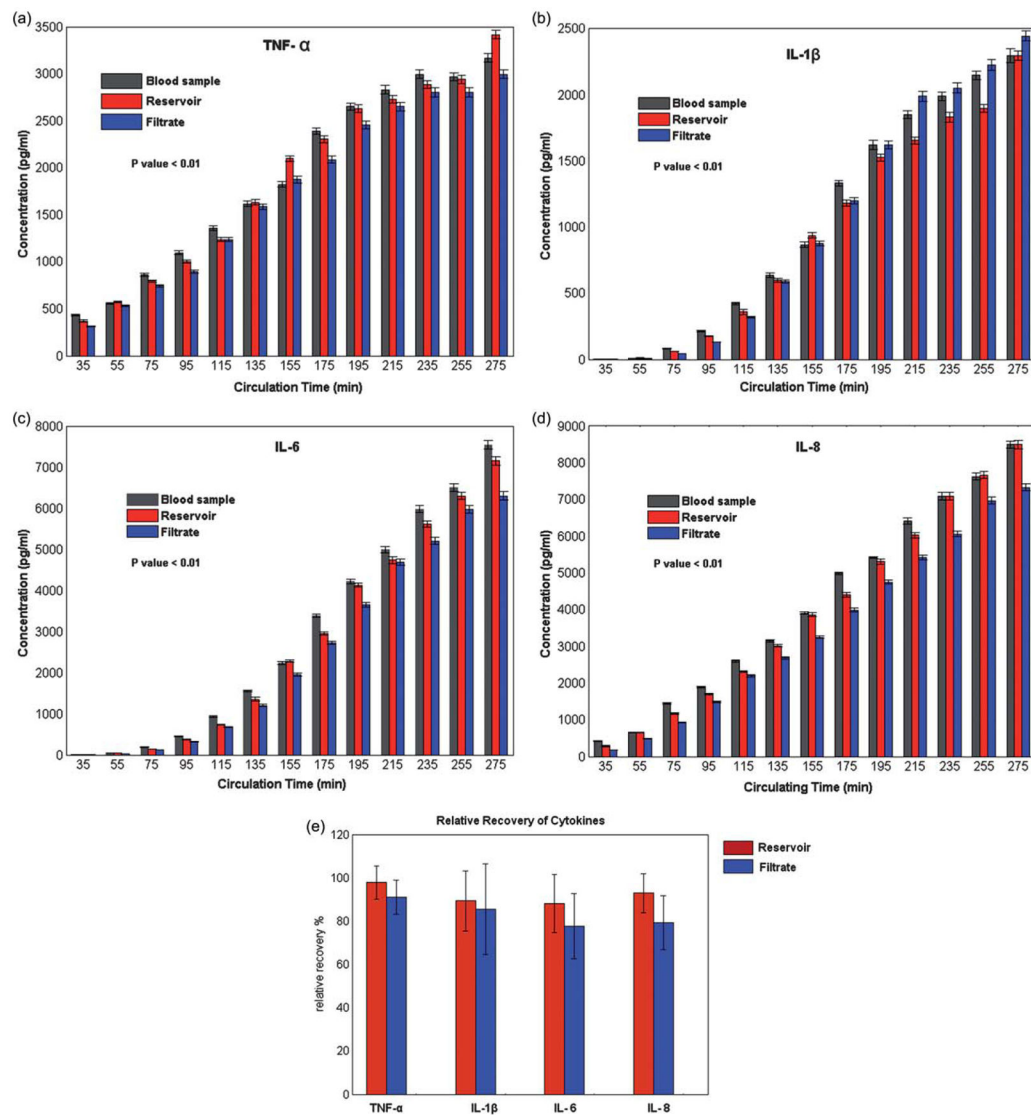


Fig. 5. (a-d) Comparison of outlet cytokine (TNF- α , IL-1 β , IL-6, and IL-8) concentrations from 13 discrete samples collected every 20 min with the microfiltration device channels (Reservoir and Filtrate) and a direct draw from the CPB membrane oxygenator arterial port (Blood Sample). The cytokine concentration increases significantly over the sampling period for each protein analyzed. The error bars represent the standard deviation of the flow cytometry bead fluorescence. (e) Average normalized recovery from the reservoir and filtration sample collected which was over 80% for all the analyzed samples.

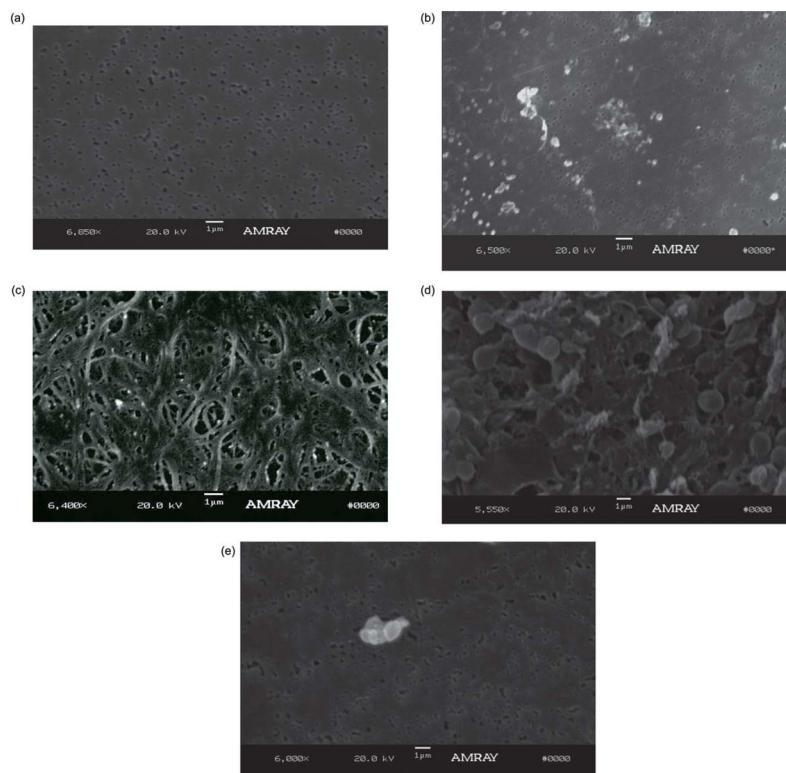


Fig. 6. Representative SEM images of porous PCTE membranes. (a) SEM images of PCTE membrane before being exposed to blood, (b) PCTE membrane after being exposed to human blood (Hct~30%). Although some protein aggregation is seen on the membrane surface after exposure to human whole blood, the underlying pores in the membrane can be clearly seen, and are not clogged. (c) PCTE membrane after being exposed to sheep blood (Hct~30%) shows significant amount of protein adhesion to membrane surface, (d) non-coated PCTE membrane after being exposed to sheep's blood (Hct = 39%) and (e) heparin coated PCTE membrane after being exposed to the same blood (Hct = 39%).

Table 1Pearson correlation coefficient, r , between microdevice samples and direct draw blood sample

Antigen	Comparison between concentrations of Reservoir and Direct Draw Sample	Comparison between concentrations of Filtrate and Direct Draw Sample
TNF- α	0.992	0.996
IL-1 β	0.996	0.997
IL- 6	0.999	0.997
IL- 8	0.997	0.998

Author Manuscript

Author Manuscript

Author Manuscript

Author Manuscript